

## **Optical humidity sensing behaviour of sol–gel processed nanostructured ZnO films**

B.C. YADAV<sup>1\*</sup>, R.C. YADAV<sup>1</sup>, G.C. DUBEY<sup>2</sup>

<sup>1</sup>Nanomaterials and Sensors Research Laboratory, Department of Physics,  
University of Lucknow, Lucknow-226007, U P, India

<sup>2</sup>Retd. Scientist ‘G’, Solid State Physics Laboratory, Lucknow Road Delhi, India

\*Corresponding author: balchandra\_yadav@rediffmail.com

This paper reports the humidity sensing behaviour of sol–gel processed ZnO films deposited on U-shaped borosilicate rods as substitute of optical fiber having the same radius of curvature. The films prepared on each sensing element were dried for 15 minutes using a 100 watt electric bulb. Both ends of the U-shaped borosilicate rod were coupled to optical fibers. Light from a He-Ne laser is fed into the sensing element through one of the ends. Light is received from the other end of fiber coupled into an optical power meter. Variations in the intensity of light with changes in humidity from 10% to 95% have been recorded. Characterization of sensing material has been done using SEM.

Keywords: humidity sensors, optical fiber, sol–gel dip process.

### **1. Introduction**

The control of humidity is becoming increasingly important for improving the quality of life and enhancing the industrial progress [1–4]. Humidity sensors based on various working principles have been produced to serve the applications. Humidity sensors based on optical methods [5–16] are best suited to those situations where remote analysis capability, high sensitivity and compactness of the device are the criteria for the measurement of humidity levels. Humidity sensors in which the sensing element is a thick or thin film have been extensively studied [5–24]. Most of these sensors are based on monitoring changes in the electrical parameters like resistance, conductance or capacitance [18–25]. Very few reports are available in which optical properties of these films are used to determine the relative humidity [7–18].

The optical humidity sensors investigated in this study consist of a thin U-shaped borosilicate-rod of 1 mm in diameter having a 7.5 mm curvature, on which a film of

ZnO is deposited. ZnO is the most advantageous metal oxide semiconductor of large band gap. It is well known for its gas sensing as well as temperature sensing behaviour. The humidity sensing behaviour of ZnO synthesized through different methods in the form of pellet was studied already by YADAV *et al.* [19–22]. In this paper, humidity sensing properties of ZnO films were investigated thoroughly by optical method using U-shaped borosilicate rod.

Modulation in the intensity of light passing through the borosilicate-rod coated with zinc oxide determines the relative humidity of the environment surrounding it. In fact, the U-shaped thin borosilicate-rod considered here would be far sturdier than either the cladded or the uncladded U-shaped optical fiber.

## 2. U-shaped borosilicate rods

Thin borosilicate rods have been bent in the shape of U, such that the separation between its two arms is given by  $2x$  and the depth of its curvature by  $y$ , as shown in Fig. 1.

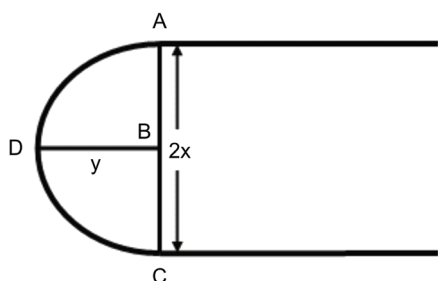


Fig. 1. U-shaped borosilicate rod used as sensing element.

Let the bend ADC of the U-shaped glass rod be the arc of the circle ADCE, as shown in Fig. 2. Also, let the radius of this circle be given by  $AO = OD = r$ , the length of the chord AC =  $2AB = 2BC$ , and the depth of curvature BD =  $r - OB = y$ . Radius

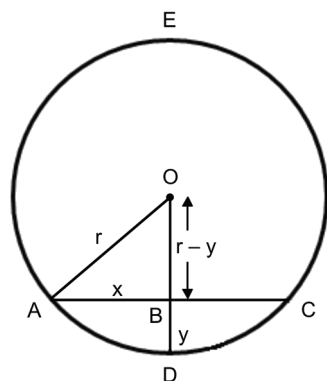


Fig. 2. Bend ADC of the U-shaped borosilicate rod as an arc of the circle ADCE.

of the bend of the U-shaped rod can then be evaluated from the geometry of Fig. 2. Therefore, from the relation

$$r^2 = OB^2 + AB^2 = (r - y)^2 + x^2 \quad (1)$$

it is found that

$$r = (x^2 + y^2)/2y \quad (2)$$

The depth of the curvature  $y$  and the separation  $2x$  between the two arms of the U-shaped glass rods of 1 mm in diameter fabricated in the laboratory have the corresponding radius of curvature  $r$  which can be evaluated with the help of Eq. (2).

### 3. Material preparation and characterization

ZnO thin films were prepared by sol-gel method. 2.5 g zinc acetate dehydrate  $Zn(CH_3COO)_2 \cdot 2H_2O$  was dissolved into 100 ml of absolute ethanol at 60 °C with constant stirring using thermo-magnetic stirrer for two hours. The obtained solution was refluxed at 100 °C for six hours in a rotary vacuum evaporator. Films were prepared on glass-slides using a spinner at 1000 rpm for 30 seconds. Surface

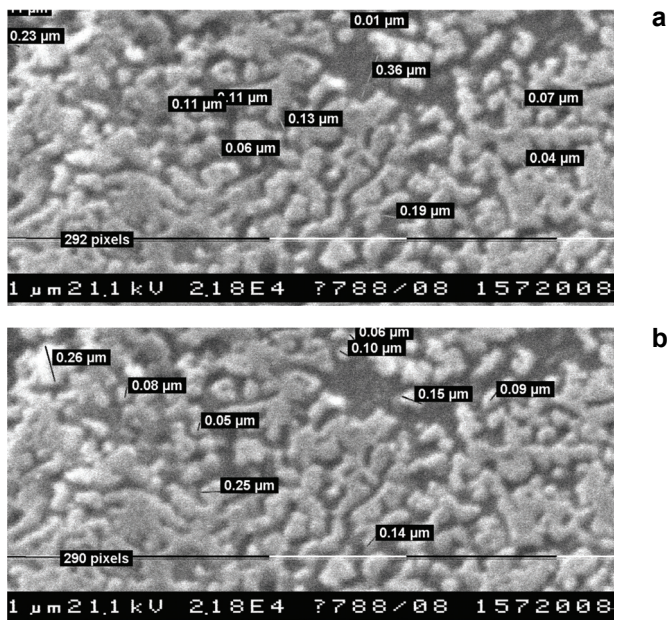


Fig. 3. Particle size of one layered film with minimum size 10 nm (a). Pore size of one layered film with max. pore size 260 nm (b).

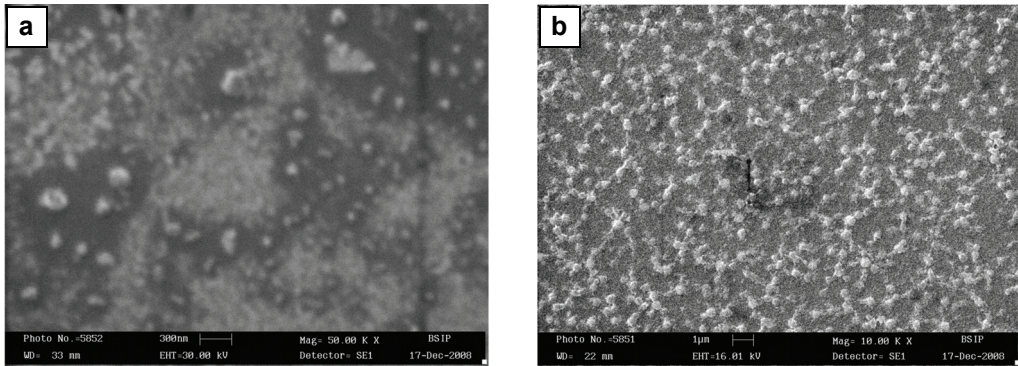


Fig. 4. Micrograph of two (a) and three (b) layered film of ZnO.

morphology of the films using scanning electron microscope (Philips 505, Netherland and Leo-0430, Cambridge) has been studied. SEM image shown in Fig. 3a reveals particle size and Fig. 3b exhibits pore size of one layered films. Figures 4a and 4b show the micrographs of two layered and three layered films of ZnO and it was found that the films are porous and sensitive to relative humidity.

#### 4. Principle of operation

The propagation of light or waveguide within an optical fiber is based on the total internal reflection (TIR). When a ray of light is incident on the interface between two dielectrics having refractive indices  $n_1$  and  $n_2$  ( $n_1 > n_2$ ) refraction occurs, which is given by

$$n_1 \sin \theta_1 = n_2 \sin \theta_2 \quad (3)$$

where  $\theta_1$  and  $\theta_2$  are the angles of incidence and refraction, respectively.

When  $\theta_2$  becomes  $90^\circ$ , the refracted ray emerges parallel to the interface between the dielectrics for which the angle of incidence is given by:

$$\sin \theta_c = n_2/n_1 \quad (\theta_c = \theta_1) \quad (4)$$

$\theta_c$  is known as critical angle. For TIR,  $\theta_1$  must be greater than  $\theta_c$ . This is the mechanism by which light at sufficiently shallow angle ( $< 90^\circ - \theta_c$ ) may be considered to propagate down an optical fiber with low loss.

Since in our experiment we used U-shaped silica glass rod fibers as a transmission medium, therefore material absorption losses as well as radiation losses mostly occur at curvatures. Due to adsorption of water molecule on the cladding surface of glass rod, refractive index increases that causes transmission losses through cladding of the fiber.

## 5. Radiation losses

There occur various radiation losses during the experiments which may be characterized as permanent and temporary losses [4, 26].

### 5.1. Material absorption losses

It is a loss mechanism related to the material composition and the fabrication process for the fiber that results in the dissipation of some of the transmitted optical power as heat in the waveguide. The absorption of the light may be intrinsic, being caused by the interaction with one or more of the major components of the glass or extrinsic due to impurities within the glass.

### 5.2. Fiber bending loss

#### 5.2.1. Macro-bending loss

Optical fibers suffer radiation losses at bends or curves on their paths. Macro-bending losses occur when the fiber cable is subjected to a significant amount of bending above a critical value of curvature. This is due to the energy in the evanescent field at the bend exceeding the velocity of light in the cladding and hence the guidance mechanism is inhibited, which causes light energy to be radiated from the fiber [4, 26].

#### 5.2.2. Micro-bending loss

It can be generated at any stage during the manufacturing process, the cable installation process or during service. Micro-bending introduces slight surface imperfections which can cause mode coupling between adjacent modes, which in turn creates a radiation loss which is dependent on the amount of applied fiber deformation, length of fiber and the exact distribution of power among the different modes.

### 5.3. Dispersion

Dispersion of the transmitted optical signal causes distortion along optical fibers because of the broadening of the transmitted light signal/pulses [4, 26]. On the basis of the dispersive mechanisms involved for the different amounts of pulse broadening within the various types of optical fibers, it is categorized as intermodal dispersion and intramodal dispersion. Pulse broadening due to intermodal dispersion results from the propagation delay differences between modes within a multimode fiber. The phenomenon of intermodal dispersion does not occur in a single mode fiber. However, intramodal (chromatic) dispersion may occur in all types of the optical fiber which results from the finite line width of the optical source. Since optical sources do not emit just a single frequency but a band of frequencies, then there may be propagation delay differences between the different spectral components of the transmitted signal. This causes the broadening of each transmitted mode and hence intramodal dispersion. The delay differences may be caused by the dispersive properties of the waveguide

material (material dispersion) and also guidance effects within the fiber structure (waveguide dispersion).

#### 5.4. Coupling loss

A greater source of optical power loss occurs at fiber–fiber connection due to misalignment of the two jointed fibers. However, when two jointed fiber ends are smooth and perpendicular to the fiber axes, and two fibers are perfectly aligned, a small proportion of the light may be reflected back into the transmitting fiber causing attenuation at the joint. This phenomenon, known as Fresnel reflection [26], is associated with the step changes in refractive index at the jointed interface. The magnitude of partial reflection of light transmitted through the interface may be estimated using the classical Fresnel formula for light at normal incidence and is given by

$$I_R = \frac{(n_1 - n_0)^2}{(n_1 + n_0)^2} \quad (5)$$

$n_1$  is the refractive index of fiber core and  $n_0$  is the refractive index of medium between two jointed fibers. Therefore, the loss will be given by (in dB):

$$\text{loss} = -10\log(1 - I_R) \quad (6)$$

### 6. Experimental details

Three U-shaped thin borosilicate rods with equal radius of curvature have been chosen. A film of ZnO is deposited on each of these glass-rods by the sol–gel dip process. Gel coated films were dried by 100 watt electric bulb for 15 minutes, and then used as sensing elements. The schematic reflection and refraction in an optical fiber attached to U-shaped borosilicate rod coated with film is shown in Fig. 5.

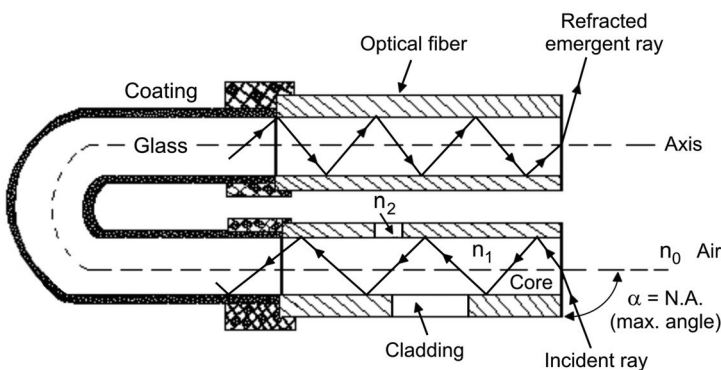


Fig. 5. Schematic diagram of reflection and refraction in an optical fiber attached to U-shaped borosilicate rod coated with film.

The experimental set-up for the sensor assembly has already been reported [3]. The U-shaped glass rod, with a ZnO film deposited on it, is fixed on the wall of a steel chamber with the help of two holes drilled in it such that the bend remains inside the chamber and the two arms protrude outside. The two ends of these arms are then coupled to plastic optical fibers. Light from an unpolarised 2 mW He-Ne laser source (OSAW, India) is launched from one of these fibers. Light received from the other fiber is fed into an optical power meter (Benchmark Model, FOPM-101) for the measurement of its intensity.

The humidity was increased from 10% to 95% by placing a saturated aqueous solution of potassium sulphate ( $K_2SO_4$ ) in a dish inside the steel chamber. The relative humidity (RH) was measured by a standard hygrometer (Huger, West Germany). The consequent changes in intensity of light emerging out of the ZnO coated U-shaped borosilicate rod were recorded for each of the thin borosilicate rods. The chamber was then dehumidified up to 10% RH by putting saturated aqueous solution of KOH inside a dish. It may be noted that on varying the humidity from 10% to 95% the temperature of the chamber decreased by 1 °C. The least count of the hygrometer used here for the measurement of RH is 1% and that of the optical power meter is 0.1 dBm.

Observations were taken for the output intensity at the one end of the U-shaped sensor, through the coupled optical fiber with the variation in the relative humidity inside the chamber. The observations for the different U-shaped humidity sensors have been plotted in Figs. 6 and 7.

## 7. Results

Variations in optical power with the variations in %RH are plotted in Fig. 6. The increase in humidity increases adsorption of water vapours and their condensation in the pores of the ZnO film causing an increase in the refractive index of the film interfacing the borosilicate rod. This leads to a greater leakage of light

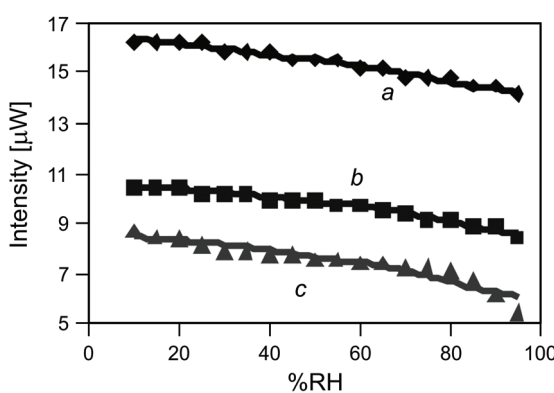


Fig. 6. Variations in the intensity of light against %RH for one (a), two (b), and three (c) layered films of ZnO on U-shaped borosilicate rods having same dimension.

through the sensing element thereby decreasing the output intensity. The sensitivity with which %RH can be measured with the help of the U-shaped humidity sensor described above is defined as:

$$S = \frac{\Delta I_r}{\Delta \text{RH}} \quad \left[ \frac{\mu\text{W}}{\% \text{RH}} \right] \quad (7)$$

where  $\Delta I_r$  is the change in intensity of transmitted light through the sensing element.

Three U-shaped borosilicate rods having identical dimension ( $r = 7.5$  mm) were taken as sensing elements. One, two and three layered films of ZnO were deposited on these elements which are denoted as *a*, *b* and *c*, respectively. Figure 6 shows the corresponding plots for this case. Curves *a*, *b* and *c* correspond to the sensing elements *a*, *b* and *c* having equal radius of curvature.

Figure 6 shows that, in general, as %RH increases the output intensity decreases. Curve *a* for sensing element coated once shows lesser slope, hence lesser sensitivity (0.022). Curve *b* for sensing element having two layered deposition of ZnO shows poor sensitivity (0.0156) than the previous sensing element. However, curve *c* for sensing element having three layered film shows highest sensitivity (0.0295) and continuous variation in output power, which is good for device fabrication.

Figure 7 shows the reproducibility of the sensing elements *a*, *b* and *c* after 24 hours. The average sensitivities of these sensing elements are  $S_a = 0.022$ ,  $S_b = 0.0156$  and  $S_c = 0.0295$ , respectively.

## 8. Discussion

It is foreseen that the increase in humidity increases adsorption of water vapour by the porous ZnO film causing a corresponding increase in its refractive index [17]. This effectively changes the boundary condition at the cladding-core interface reducing

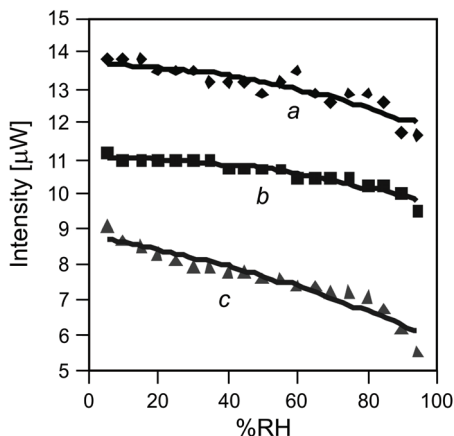


Fig. 7. Reproducibility of results of the sensing elements *a*, *b* and *c* after 24 hours.

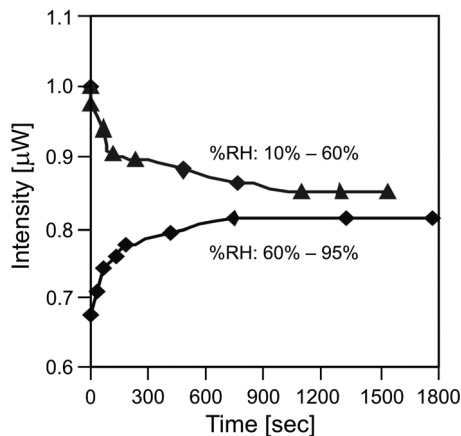


Fig. 8. Response and recovery curve.

the beam confinement in the guide, thereby reducing the light intensity emerging through the ZnO cladded thin borosilicate rod. To start with, the ZnO film is free of water molecules and has dry air in its pores. On being exposed to environment of lower humidity, rapid surface adsorption of water vapours into the porous film begins, causing rapid attenuation of the light propagating through the ZnO cladded thin borosilicate rod. This attenuation may be attributed to the increased leakage of light in to the cladding of the rod, the refractive index of which increases as the RH increases. Therefore, the sensitivity is higher in this region. In the higher RH range, the capillary condensation occurs and forms a meniscus in the capillaries of the cladding. The attenuation of light and hence the sensitivity starts decreasing in this range of %RH. As the %RH increases further the porous ZnO film starts becoming saturated resulting in a still smaller sensitivity for this region. The response and recovery times for the sensor element *c* are 120 and 195 sec, respectively, as shown in Fig. 8. The response of the sensors observed here can be attributed to the fast penetration of water molecules into the cladding. The slower recovery in the response, on the other hand, is caused by a slow desorption process and capillary forces.

## 9. Conclusions

The results described above clearly show that the optical humidity sensors can be used to measure %RH in the broad range of 10%–95%. These sensors are characterized by reliability and cost-effectiveness. This investigation has impact on the development of fiber optical humidity sensor which can perform accurate measurement even at remote and unmanned stations.

*Acknowledgement* – We acknowledge the Uttar Pradesh Council of Science and Technology, Lucknow for financial support in the form of Project.

## References

- [1] KULWICKI B.M., *Humidity sensors*, Journal of the American Ceramic Society **74**(4), 1991, pp. 697–708.
- [2] CHEN ZHI, LU CHI, *Humidity sensors: A review of materials and mechanisms*, Sensor Letters **3**(4), 2005, pp. 274–295.
- [3] TRAVERSA E., *Ceramic sensors for humidity detection. The state of the art and future developments*, Sensors and Actuators B: Chemical **23**(2–2), 1995, pp. 135–156.
- [4] GUPTA B.D., *Fiber Optic Sensors – Principal and Applications*, 1st Edition, New India Publishing Agency, New Delhi 2006, pp. 1–10, 21–28, 92–98.
- [5] EISENBERG D., KAUFMANNS W., *The Structure and Properties of Water*, Oxford University Press, 1969.
- [6] MORIMOTO T., NAGAO M., TOKUDA F., *Relation between the amounts of chemisorbed and physisorbed water on metal oxides*, Journal of Physical Chemistry **73**(1), 1969, pp. 243–248.
- [7] OGAWA K., TSUCHIYA S., KAWAKAMI H., TSUTSUI, T., *Humidity-sensing effects of optical fibres with microporous  $SiO_2$  cladding*, Electronics Letters **24**(1), 1988, pp. 42–43.
- [8] BROOK T.E., TAIB M.N., NARAYANASWAMY R., *Extending the range of fibre-optic relative-humidity sensor*, Sensors and Actuators B: Chemical **39**(1–3), 1997, pp. 272–276.
- [9] KHARAZ A., JONES B.E., *A distributed optical-fibre sensing system for multi-point humidity measurement*, Sensors and Actuators A: Physical **47**(1–3), 1995, pp. 491–493.
- [10] WALBRAN S., KORNYSHEV A.A., *Proton transport in polarizable water*, Journal of Chemical Physics **114**(22), 2001, p. 10039.
- [11] BALI L.M., YADAV B.C., DUBEY G.C., SRIVASTAVA R.K., SRIVASTAVA A., SINGH R.N., *Optical humidity sensors*, 7th National Seminar on Physics & Technology of Sensors, Pune, India 2007, pp. C.35.1–C.35.6.
- [12] YADAV B.C., *Sol-gel processed titania films on a prism substrate as an optical moisture sensor*, Sensors and Transducers Journal **79**(5), 2007, pp. 1217–1224.
- [13] YADAV B.C., PANDEY N.K., SRIVASTAVA A.K., SHARMA P., *Optical humidity sensors based on titania films fabricated by sol-gel and thermal evaporation methods*, Measurement Science and Technology **18**(1), 2007, pp. 260–264.
- [14] YADAV B.C., SHUKLA R.K., BALI L.M., *Sol-gel processed  $TiO_2$  films on U-shaped glass-rods as optical humidity sensor*, Indian Journal of Pure and Applied Physics **43**(1), 2005, pp. 51–55.
- [15] SHUKLA S.K., PARASHAR G.K., MISHRA A.P., MISRA P., YADAV B.C., SHUKLA R.K., BALI L.M., DUBEY G.C., *Nano-like magnesium oxide films and its significance in optical fiber humidity sensor*, Sensors and Actuators B: Chemical **98**(1), 2004, pp. 5–11.
- [16] YADAV B.C., SHUKLA R.K., *Titania films deposited by thermal evaporation as humidity sensor*, Indian Journal of Pure and Applied Physics **41**(9), 2003, pp. 681–685.
- [17] DIXIT S., SRIVASTAVA A., SRIVASTAVA A., SHUKLA R.K., *Sol-gel derived zinc oxide films and their sensitivity to humidity*, Japanese Journal of Applied Physics, Part 1, **47**(7), 2008, pp. 5613–5618.
- [18] DIXIT S., SRIVASTAVA A., SHUKLA R.K., SRIVASTAVA A., *Pulsed laser deposited  $ZnO$  films and their humidity sensing behavior*, Journal of Materials Science: Materials in Electronics **19**(8–9), 2008, pp. 788–792.
- [19] YADAV B.C., SRIVASTAVA R., DWIVEDI C.D., PRAMANIK P., *Moisture sensor based on  $ZnO$  nanomaterial synthesized through oxalate route*, Sensors and Actuators B: Chemical **131**(1), 2008, pp. 216–222.
- [20] YADAV B.C., SRIVASTAVA R., DWIVEDI C.D., *Synthesis and characterization of  $ZnO-TiO_2$  nanocomposite and its application as humidity sensor*, Philosophical Magazine **88**(7), 2008, pp. 1113–1124.
- [21] SRIVASTAVA R., YADAV B.C., DWIVEDI C.D., KUMAR R., *Comparative study of moisture sensing properties of  $ZnO$  nanomaterials through hydroxide route by mixing dropwise and sudden*, Sensors and Transducers Journal **80**(6), 2007, pp. 1295–1301.

- [22] YADAV B.C., SRIVASTAVA R., DWIVEDI C.D., *Synthesis and characterization of ZnO nanorods by the hydroxide route and their application as humidity sensors*, Synthesis and Reactivity in Inorganic, Metal-Organic and Nano-Metal Chemistry **37**(6), 2007, pp. 417–423.
- [23] YADAV B.C., SRIVASTAVA A.K., SHARMA P., *Resistance based humidity sensing properties of TiO<sub>2</sub>*, Sensors and Transducers Journal **81**(7), 2007, pp. 1348–1353.
- [24] YADAV A.K., YADAV B.C., SINGH K., *Solid-state conductivity of sucrose and its applications as humidity and temperature sensors*, Sensors and Transducers Journal **88**(2), 2008, pp. 66–73.
- [25] YADAV B.C., SHARMA P., SRIVASTAVA A.K., YADAV A.K., *Synthesis of antimony doped tin oxide and its use as electrical humidity sensor*, Sensors and Transducers Journal **92**(5), 2008, pp. 99–107.
- [26] SENIOR J.M., *Optical Fiber Communications*, 2nd Edition, Prentice-Hall of India Private Limited, New Delhi 2004, pp. 212–214.

Received December 23, 2008  
in revised form February 22, 2009